https://doi.org/10.32762/eygec.2025.3

GENERALIZED INTERPOLATION MATERIAL POINT METHOD REPLICATION OF VIBRATIONS CAUSED BY DYNAMIC COMPACTION

Naum SHPATA¹², Piotr KANTY³, Wojciech T. SOŁOWSKI⁴

ABSTRACT

The study attempts to replicate vibration data caused by dynamic compaction with the Generalized Interpolation Material Point Method. The paper simulates dynamic compaction based on data from a case study from Gda sk, Poland. We used the Mohr-Coulomb constitutive model with manually adjusted stiffness to account for the nonlinear small-strain stiffness of soil. The findings reveal errors ranging from 0% to approximately 50% in maximum vertical acceleration compared to measurements. However, the peak vertical velocities align well with empirical estimates and Finite Element Method simulations. These results highlight the potential of the Material Point Method for vibration analysis while underlining the need for further refinement to enhance accuracy.

Keywords: material point method, dynamic compaction, vibrations.

INTRODUCTION

This paper shows a simulation with the Generalised Interpolation Material Point Method (GIMP) aiming at the replication of vibrations at significant distances resulting from dynamic compaction. Dynamic compaction (Ménard & Broise 1975) is a soil improvement technique primarily used for granular materials. The process involves densifying the soil through high-energy impacts delivered by a heavy tamper. An inevitable consequence of this process is the generation of vibrations, as investigated numerically e.g. by Pan & Shelby (2002) and Mehdipour & Hamidi (2017). During the dynamic compaction process, the strain levels near impact are very high, while further away, the shear strain falls into the small and very small strain ranges, as defined by Burland (1989) and Ishihara (1996). In the small strain range the soil is much stiffer than at larger strains occurring near the impact of the tamper. The stiffness increase is highly non-linear and strain-dependent. A comprehensive constitutive model for soil should account for both soil densification (volume change) and the dynamic behaviour of the material. However, such models often require numerous parameters, which may be unavailable. As a result, geotechnical engineers frequently rely on simpler models for their predictions. This paper parametrises the Mohr-Coulomb model to capture high stiffness in the small strain range to obtain a realistic replication of measured vibration.

The framework is developed within the Generalized Interpolation Material Point Method (GIMP). The ability of GIMP to simulate the Dynamic Compaction

process was demonstrated by Sołowski et al. (2013). GIMP, originally introduced by Bardenhagen & Kober (2004), discretises a continuum with material points that have defined domains. All the domains of material points together cover the whole body of the material.

This study uses the uniform/unchanged GIMP (uGIMP) variant, where the control domain retains its initial shape. The goal is to evaluate the current capabilities and limitations of uGIMP for practical engineering applications related to vibration prediction from Dynamic Compaction.

METHODOLOGY

This work focuses on predicting vibrations at a distance, rather than close to the impact point. as existing structures sensitive to vibrations are usually located tens or hundreds of meters away from the impact. Furthermore, an additional purpose of this case study is to help to evaluate the potential limitations of the GIMP computational framework in the replication of vibrations. The simulated case study is based on dynamic compaction ground improvement made in Gda sk by Menard Group. The details of the case are available in the thesis of Shpata (2024). In the simulation, the simplified soil profile consists of three (3) parallel layers: two types of sand (Sand1 and Sand2) and a bottom layer of silty sand. Table 1 gives the maximum ($G_{max,max}$) and minimum ($G_{max,min}$) estimation of the small strain shear moduli (G...) for each layer.

¹ Doctoral Researcher, Aalto University, 02150 Espoo, Finland, naum.shpata@aalto.fl

² Corresponding author

³ R&D Director, Menard Sp z o.o, 00-203 Warszawa, Poland, pkanty@menard.pl

⁴ Associate Professor, Aalto University, 02150 Espoo, Finland, wo joiech.solowski@aalto.fl

Table 1 Initial vs. Final Void Ratios

Soil Type	Depth [m]	G _{max,min} [MPa]	G _{max,max} [MPa]
Sandi	0-4	27	65
Sand2	4-8	51	145
Silty Sand	8-10	9	25

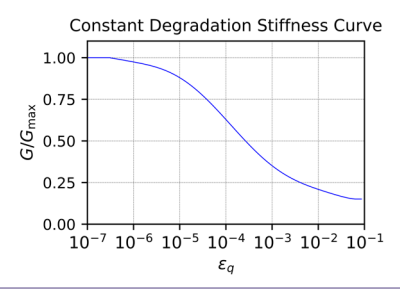


Figure 1 Constant Degradation Stiffness Curve

Since soil stiffness varies with strain levels, the simulation identifies areas with similar deviatoric shear amplitude (ϵ_a) and then assigns the stiffness according to the degradation curve shown in Figure 1. The distribution of the areas is shown in Figure 2. A similar method was used by Quintero Martinez (2022), Ruan (2023) and Shpata (2024). Such an approach efficiently parametrises elastoplastic models with linear elasticity, such as the Mohr-Coulomb model, to incorporate small strain behaviour. However, it relies on extensive manual work and carries a risk of human error during domain discretization. Also, it does not replicate the whole degradation curve and cannot accurately predict other complex features of soil behaviour in the small strain range. The domain was divided into four areas based on distance (d) from the centre of the simulation (0.0) along the axis of symmetry (Figure 2). The deviatoric strain level determines the shear modulus (G) using the stiffness degradation curve, Figure 1. Then, bulk modulus is computed with Equation 1 under the assumption of a constant Poisson's ratio (ν).

$$K = \frac{2G(1+v)}{3(1-2v)} \tag{1}$$

Table 2 presents the maximum and minimum shear modulus values for the three layers.

The computational framework employs the Generalized Interpolation Material Point Method (GIMP) as coded in the open-source Uintah code, see e.g. Guilkey et al. (2009). The simulation assumes axisymmetry. The domain of size 102x17 m is discretised by 0.5x0.5 m material point domains, resulting in 4896 points (Figure 2). Since Uintah lacks absorbing boundaries, which are essential for preventing numerical wave reflections, a viscoelastic Kelvin-Voigt material (see Table 3 for parameters) is applied at the bottom (y_{min}) and the end (x_{max}) of the domain. This model combines a spring and a dashpot in parallel. The viscous properties $(\eta_G$ and $\eta_K)$ were tuned to be close to critical values (Equation 2) to avoid overdamping and underdamping of the system. They are estimated based on mass/density (m) and stiffness (K and G).

Table 2 Initial vs. Final Void Ratios

ε q	<10-6.5	<10-5	<10-4	>10-2
d	78-100	48-78	20-48	0-20
G _{min,min} (MPa)				
Sand1	27	24	17	6
Sand2	51	45	32	11
Silty Sand	9	8	6	2
G _{max,max} (MPa)				
Sand1	65	57	41	14
Sand2	145	128	91	30
Silty Sand	25	22	16	5

$$\eta_G = 2\sqrt{mG}; \eta_K = 2\sqrt{mK} \tag{2}$$

Table 3 Visco-Elastic Absorbing Layer properties

Visco-Elastic Absorbing Layer			
Density (kg/m³)	1937		
Elastic Bulk Modulus (K) (MPa)	500		
Elastic Shear Modulus (G) (MPa)	1083		
Viscous Bulk Modulus (ηK) (kPa*s)	1968		
Viscous Shear Modulus (ηG) (kPa*s)	2897		

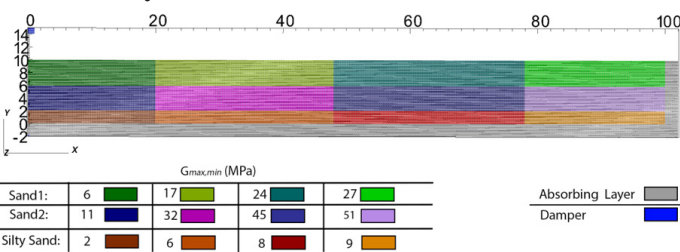


Figure 2 Initial Configuration of the domain (4896 points)

Uintah software lacks the ability to define initial conditions with gravity with zero displacements. Hence, gravity induces elastic deformations and vibrations when the soil is at rest. The resulting numerical noise ranges between 0.1 - 0.5 m/s and fluctuates over time. As we use no numerical damping in the simulation, these elastic waves do not disappear over time. Such vibrations might be negligible in some simulations, yet they are dominant when the expected velocities at a distance are only 1-2 mm/s. We have failed to reduce the noise with a number of numerical techniques, including ramping gravity linearly and non-linearly over time and applying high artificial damping initially, then reducing it to zero.

The presented solution relies on the superposition principle. Equation 3 describes this approach: the estimated vertical velocity (v_y) at distance d is the difference between the simulated velocity with both gravity and impact (v_{yy}) and the velocity from the gravity-only simulation (v_{yy}) .

$$v_y = v_{y,gi} - v_{y,g} \tag{3}$$

Observations from engineering practice reveal that pre-impact velocity deviates from free-fall theory, showing lower amplitudes. Data from the tamper falls of approximately 5 m and 10 m heights provided acceleration signals. Numerical integration of these signals produced velocities of 9.4 m/s for a 5 m fall and 12.5 m/s for a 10 m fall, both lower than the theoretical free-fall estimates of 9.9 m/s and 14.5 m/s, respectively. The mentioned velocities were used for the simulations. The tamper is simulated utilizing the Mohr-Coulomb model with high stiffnesses and dimensions of 1x1 m.

RESULTS

Four cases were analysed: two with a falling height of 5 meters and two with a height of 10 meters. For each height, one case used the minimum small strain shear modulus ($G_{\max,\min}$), while the other utilized the maximum small strain shear modulus ($G_{\max,\max}$). The resulting vertical velocity at 50 meters is presented in Figure 3.

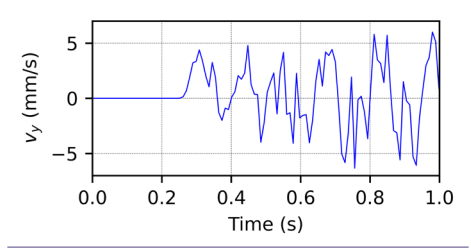


Figure 3 Vertical velocity at a 50m distance for the case of Gmax,max and 10 m drop height

The graph shows that the superposition principle holds only for the first peaks following the impact. The first peak is defined as the peak before the curvature changes significantly. This

means a change in sign on the derivative or the derivative decreases by an order of magnitude. As the point moves significantly, gravity's influence deviates from the initial state (before impact), leading to altered oscillations that invalidate the superposition principle.

Comparing these results to in situ measurements presents challenges. The experiment recorded acceleration data. Hence, the maximum derivative of the velocity over time (slope of the steepest part-reference line) was calculated to determine the maximum acceleration (a_y) (see Figure 4), while Table 4 presents the comparison with the field data

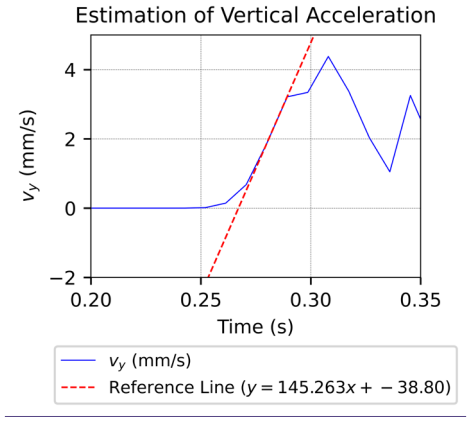


Figure 4 Estimation of vertical acceleration based on uGIMP result for the case of G_{\max} and falling height of 10 m

Table 4 Comparison of vertical accelerations for falling heights of 5m and 10m.

Vertical Acceleration (a _y) (m/s²)				
Cases		Field	MPM	ξ
5m	G _{max,min}	0.120	0.063	48
	G _{max,max}		0.100	17
10m	G _{max,min}	0.145	0.089	39
	G _{max max}		0.145	0

^{*}E. Percentage error between the uGIMP result and field measurement.

The maximum vertical velocities were also compared to peak values from validated Finite Element Method (FEM) simulations (Shpata, 2024) and empirical limits from Kirsh & Bell (2012), as summarized in Table 5.

Table 5 Comparison of vertical velocities for falling heights of 5m and 10m

Vertical Velocities (v _y) (mm/s)					
Cases		MPM	FEM	η	
5m	G _{max,min}	1.9	1.75	8	
	G _{max,max}	2.2	2.00	10	
10m	G _{max,min}	2.7	2.75	2	
	G _{max,max}	3.25	2.75	18	

Empirical expected values: 0-8 mm/s at 50 m from the impact. The results are within the expected range.

 $\eta\textsc{:}$ The percentage deviation between the uGIMP model result and the PLAXIS result.

CONCLUSION

This research work presented a methodology within the Material Point Method to estimate vibrations. The study employed the Mohr-Coulomb model and incorporated the non-linear stress-strain relationship at small strains. The final estimation of vibration used the superposition principle to remove noise from gravity. Calculations using Gmax,max show good accuracy with a maximum error of 17%. However, uncertainty is higher in cases with Gmax,min where the errors range from 38% to 48%. Results align reasonably with empirical estimates, staying within expected limits. The maximum 18% deviation compared to the validated FEM analysis seems to be reasonable taking into account the simplicity of the simulation.

It seems that the Material Point Method framework, particularly uGIMP, shows promise for simulating dynamic compaction and the resulting vibrations. Yet, as demonstrated in this study, further development is necessary. Key issues to tackle include the viscous boundaries and gravity-induced noise. Additionally, the use of a more advanced model incorporating the small-strain stiffness degradation curve and material damping would likely enhance the accuracy of the results and reliability of the obtained predictions.

ACKNOWLEDGMENTS

This research was funded by two projects: DeMiCo, supported by Decarbonized Cities Business Finland financing, and Compactit, funded by the Research Council of Finland, decision number 349755. We also thank the Menard Group for providing field data from their projects.

REFERENCES

- Bardenhagen, S. G., & Kober, E. M. (2004). The generalized interpolation material point method. Computer Modeling in Engineering and Sciences, 5(6), 477-496.
- Burland, J. B. (1989). Ninth Laurits Bjerrum Memorial Lecture: "Small is beautiful"—the stiffness of soils at small strains. Canadian Geotechnical Journal. 26(4): 499-516.https://doi.org/10.1139/t89-064
- Guilkey, J., Harman, T., Luitjens, J., Schmidt, J., Thornock, J., de St Germain, J. D., ... & Humphrey, A (2009). Uintah user guide. Scientific Computing and Imaging Institute, University of Utah, Salt Lake City, UT, USA, Tech. Rep. No. UUSCI-2009-007
- Ishihara, K. (1996). Soil behaviour in earthquake geotechnics. Oxford University Press.
- Kinsch, K., & Bell, A. (Eds.). (2012). Ground Improvement (3rd ed.). CRC Press. https://doi.org/10.1201/ b13678
- Mehdipour, S., & Hamidi, A. (2017). Impact of tamper shape on the efficiency and vibrations induced during dynamic compaction of dry sands by 3D Finite Element modeling. Civil Engineering Infrastructures Journal, 50(1), 151-163.
- Pan, J. L., & Selby, A. R. (2002). Simulation of dynamic compaction of loose granular soils. Advances in Engineering Software, 33(7-10), 631-640. https:// doi.org/10.1016/S0965-9978(02)00067-4
- Quintero Martinez, A. (2022). Assessment of the values of dynamic factors based on data from the Kokemäki-Pori railway section. MSc thesis, Aalto University. Available at: https://urn. fl/URN:NBN:fisalto-2022/0165940, accessed: 27/03/2025.
- Ruan, C. (2023). Towards high-speed railwayeffects on nearby structures and estimation of ballast degradation. MSc thesis, Aalto University. Available at: https://urn.fl/ URNNBN:fizalto-2023/0156349, accessed: 27/03/2025.
- Shpata, N. (2024). Numerical replication of vibrations caused by dynamic compaction. MSc thesis, Aalto University. Available at: https://urn.fl/URN:NBN:fl:aalto-202408255700, accessed: 27/03/2025.
- Solowski, W. T., Sloan, S. W., Kanty, P. T., & Kwiecien, S. (2013). Numerical simulation of a small scale dynamic replacement stone column creation experiment. PARTICLES III: Proceedings of the III International Conference on Particle-Based Methods: Fundamentals and Applications, 522-533.